DOI:
10.1039/C9MH01496A

Document Version
Peer reviewed version

COMMUNICATION

Expanding the design space of gel materials through ionic liquid mediated mechanical and structural tuneability

Received 00th January 20xx,
Accepted 00th January 20xx

DOI: 10.1039/x0xx00000x

Alex P. S. Brogan,*[a,b] Coby J. Clarke, [b] Artemis Charalambidou, [b] Colleen N. Loynachan,[c] Sarah E. Norman,[d] James Doutch[e] and Jason P. Hallett.[b]

Ionogels are an emerging class of soft material with exceptional properties stemming from high ionic liquid content. In contrast to other gel systems, the ionic liquid component provides an extra level of design. However, this highly modular nature has yet to be fully explored and the role ionic liquids play in the structural properties of gel-based materials is poorly understood. Here, methodical small angle neutron scattering and X-ray photoelectron spectroscopy studies reveal the relationship between bulk structure and surface composition of a soft material for the first time. Furthermore, we show how ionic liquid design dictates polymer structure, which in turn can be harnessed to fine tune the mechanical properties of ionogels. With a level of control over gel structure beyond what is possible using molecular solvents, our systematic study thus provides insight into how ionic liquids can expand the design space for gel development for a broad range of applications.

Ionogels are a new class of soft material typically consisting of ionic liquid encapsulated within a polymer matrix. In comparison to their hydrogel (water-based gel) and organogel (organic solvent-based gel) counterparts, ionogels have many favourable properties stemming from the ionic liquid component. These organic salts have low melting temperatures, typically below 100 °C and frequently around room temperature, and are increasingly popular solvents with attractive properties such as; ion conductivity, thermal stability, and negligible vapour pressure.[1,2] The latter attribute being of particular interest for material design as the gels never dry out and thus functional properties are easier to maintain for longer periods. As such, ionogels are promising materials for a host of applications.[3–5] Most notably in the current literature they are being explored predominately as new materials for flexible batteries and soft electronics.[6–15] Additionally, ionic conductivity and broad chemical and electrochemical stability make them promising materials for interfacing with biology[16], for prospective uses in biocatalysis[17], biosensing devices, and soft robotics.

A key advantage of ionogels over hydrogel and organogels is that ionic liquids have highly tuneable chemical and physical properties, a result of the near endless combinations of anions and cations that result in room temperature liquids. The consequence of which is that ionogels, by their very nature, are incredibly modular materials.[11,14,18] Polymer composition and concentration, crosslinking strategy, and both ionic liquid anion and cation can be individually and systematically interrogated to achieve desired material properties. Despite this, current studies have been limited to assessing ionogels as task specific, single polymer-ionic liquid pairings. To date, there has been no systematic study to fully investigate controlling the modularity of these materials through the interplay between ionic liquid and gel structure: arguably the truly unique feature of ionogels in comparison to other gel systems. As the ionogel field matures, with recent reports of ionogels with ever more complex functions such as self-oscillating actuation[19], peristaltic crawling[20], and therapeutic delivery[21] there is an increasing requirement to understand how to control, and thus design, ionogels with specific structural motifs and predetermined mechanical properties. Key to this will be understanding the gel structure within ionic liquids, through a comprehensive study of ionic liquid induced polymer structuration.

Here, we systematically explore how ionic liquid selection can dictate gel properties. Specifically, the stress-strain relationships of ionogels containing photo-crosslinked poly(ethylene glycol) diacrylate [PEGDA] at varying concentrations, with ionic liquids of differing anion basicity (β) were investigated. The unique properties of ionogels allowed for the elucidation of polymer structure within the gels using

[a] *Department of Chemistry, King's College London, Britannia House, London, SE1 1DB, UK.*
[b] *Department of Chemical Engineering, Imperial College London, London, SW7 2AZ, UK.*
[c] *Department of Materials, Imperial College London, London, SW7 2AZ, UK.*
[d] *ISIS Deuteration Facility, ISIS Neutron and Muon Source, STFC, Harwell Science and Innovation Campus, Didcot, Oxfordshire OX11 0QX, UK.*
[e] *ISIS Neutron and Muon Source, STFC, Harwell Science and Innovation Campus, Didcot, Oxfordshire OX11 0QX, UK.*

Electronic Supplementary Information (ESI) available: Containing Materials and Methods, additional data tables, and XPS scans. See DOI: 10.1039/x0xx00000x

SANS, coupled with an unprecedented X-ray photoelectron spectroscopy (XPS) examination of the surface composition of the gel materials. Thus providing a comprehensive structural basis for how ionic liquid influences gel structure and how that in turn affects mechanical stability. In doing so, we found that ionogel strength was inversely correlated to the polarity of the anion of the ionic liquid. The less polar ionic liquids were better solvents for PEGDA, resulting in ionogels with increased strength and toughness. This study therefore provides the basis for understanding how ionic liquids can be used to expand the design space of gel materials for a broad range of applications.

Results and Discussion

Thermally robust self-supporting ionogels were observed in all of the ionic liquids tested, at PEGDA concentrations ranging from 10 to 40 wt%. Polymer concentrations less than 10 wt% produced viscous fluids rather than self-supporting gels, indicating that 10 wt% PEGDA was the minimum polymer concentration required for ionogel fabrication under ambient conditions, where the presence of oxygen and water vapour (*ca.* 2 wt% of final gel) may impede successful photocrosslinking, as oxygen is an effective inhibitor of radical polymerizations.[14] As

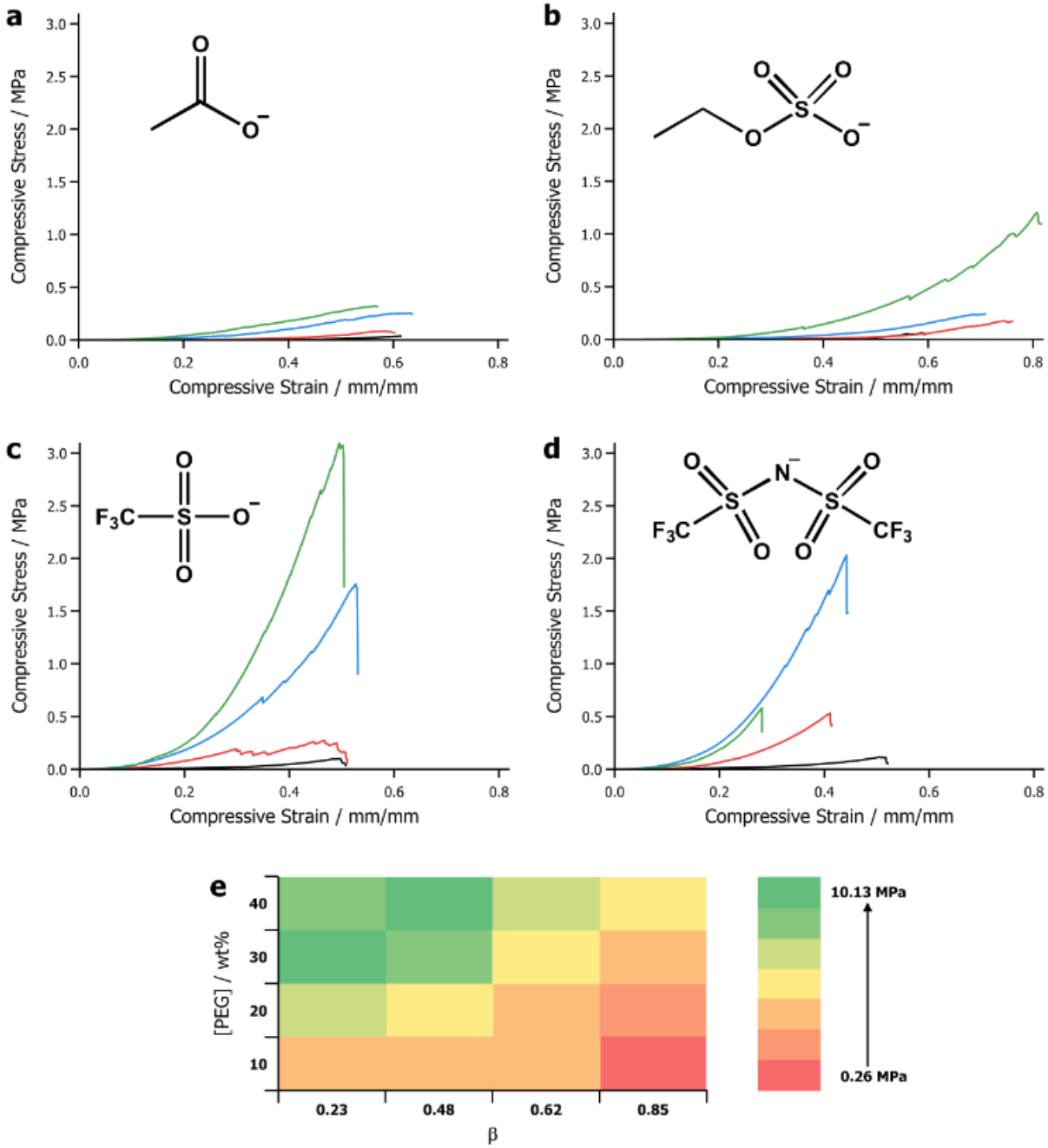

Figure 1. (**a** – **d**) Plots of compressive stress against compressive strain for ionogels of [emim][OAc] (**a**), [emim][$EtSO_4$] (**b**), [emim][OTf] (**c**), and [emim][NTf_2] (**d**) with PEGDA concentrations of 10 wt% (black), 20 wt% (red), 30 wt% (blue), and 40 wt% (green). Insets show ionic liquid anion structure. (**e**) Qualitative heat map showing compressive modulus at high strain as an indicator of gel stiffness with respect to polymer concentration and anion basicity (β), where red represents the most flexible gel (lowest modulus) and green represents the stiffest gel (highest modulus).

a result, lower polymer concentrations were not taken forward for further analysis in this study. One of the more desirable properties of ionic liquids, particularly over conventional molecular solvents, is the ability to tune their solvent properties simply by exchanging the components of the salt. The anion significantly affects the polarity of the ionic liquid, and how interacting the ionic liquid is towards solutes[22,23], particularly impacting the solubility of macromolecules[24]. Whilst the cation has also been shown to aid in the solvation of ethylene oxide polymers through hydrogen bonding[25], for clarity, we decided to vary the anion and fixed the cation as the commonly used 1-ethyl-3-methylimidazolium (emim), with cation dependence the subject of future investigations. Anion basicity can broadly be quantified through the Kamlet-Taft parameter for hydrogen bond basicity: β.[22] To investigate the effect of altering the polarity of the ionic liquid on the resultant gel phase properties, we therefore chose anions that covered a broad range of β values, ranging from the highly interacting and polar anion acetate (OAc, β = 0.85)[23] through to the largely non-interacting and hydrophobic anion bis(trifluoromethylsulfonyl)imide (NTf_2, β = 0.23)[23] [SI Table 1].

The key physical property of self-supporting gels with respect to future device-based applications is their mechanical properties. Therefore, we sought to investigate how ionic liquid and polymer content could be used as parameters to fine tune the stiffness and toughness of the resultant ionogels. For this, we performed compressive stress-strain tests on the gels to evaluate their compressive modulus at both low and high strain (as a measure of stiffness) and failure stress (as a measure of toughness) (Fig. 1, SI Table 2). Given that the gels presented fairly complex viscoelastic behaviour, for simplicity, we chose to discuss the following in terms of the compressive modulus at high strain as a measurement of maximum stiffness. For [emim][OAc] gels (Fig. 1a), increasing crosslinked PEGDA concentration from 10 to 40 wt% increased the compressive modulus of the gels from 0.26 MPa to 1.18 MPa and the failure stress from 0.08 MPa (at 20 wt%, no measurable failure was observed for 10 wt% gels) to 0.54 MPa (SI Table 2). Similarly, increasing PEGDA concentration from 10 to 40 wt% in [emim][$EtSO_4$] gels increased the compressive modulus from 0.77 MPa to 4.16 MPa, and failure stress from 0.06 MPa to 1.11 MPa (Fig. 1b). Thus, increasing the polymer concentration by a factor of 4, increased the stiffness and strength of the resultant ionogels up to 5-fold. For [emim][OTf] (Fig. 1c) and [emim][NTf_2] ionogels (Fig. 1d) failure was detected by a sharp transition in the stress strain response, a parameter that was less evident for the [emim][OAc] and [emim][$EtSO_4$] ionogels. This suggested that although increasing polymer content increased the compressive modulus of the gels (increasing from 0.75 MPa up to 10.13 MPa – a 13-fold improvement in strength), increased toughness came at a cost of increased brittleness (failure strain was consistently lower for the [emim][OTf] and [emim][NTf_2] ionogels than the [emim][OAc] and [emim][$EtSO_4$] ionogels – SI Table 2). Additionally, the basicity of anion provided further control over gel mechanical properties, where decreasing β increased gel stiffness at all polymer concentrations (summarized in Fig. 1e). This was the case for all of the ionic liquids, except for [emim][NTf_2] gels (Fig. 1d), where the 40 wt% gel had a lower compressive modulus (8.29 MPa) and failure stress (0.9 MPa) than the corresponding 30 wt% gel (10.13 MPa and 1.58 MPa respectively – SI Table 2). In this case, the gel was so brittle that strength was compromised, aptly characterised by a dramatic drop in failure strain from 43 % strain at 30 wt% to 27 % strain at 40 wt% (SI Table 2).

The mechanical properties of the ionogels demonstrated that there was a strong correlation with anion basicity and gel stiffness. Notably, for crosslinked PEGDA ionogels, compressive modulus was inversely proportional to anion basicity (Fig. 1e). We initially hypothesized that ionic liquid with higher β values would act as better solvents for the polymer, improving cohesion and resulting in a tougher gel. Instead, the crosslinked PEGDA ionogels exhibited an inverse gel strength relationship to the solvent polarity. This was not necessarily unexpected, as PEG, although notable for favourable interactions with water, is not regarded as a polar polymer.[26] Ionic liquid-polymer solvent pairing - matching the polarity of the ionic liquid such that it is a better solvent for the polymer - has a significant impact on the subsequent ionogel properties: thus providing the basis for an additional level of control over mechanical properties beyond what is possible through varying polymer loading alone in conventional gel systems with a single solvent.

To date, small angle neutron scattering (SANS) has been performed on a limited set of ionogels to study polymer structure.[27–29] In light of the apparent solvent dependency on ionogel mechanical strength, we hypothesized that a comprehensive SANS study could elucidate whether polymer structure was driving ionogel properties. To investigate this effect further, scattering profiles were collected for all the crosslinked ionogels (10 – 40 wt% PEGDA) with corresponding solutions of ionic liquid and (uncrosslinked) 5 wt% PEGDA for reference (Fig. 2a,c,e,g). Plots were fitted with a correlation length function, where the porod exponent (n, used as a measure of how compact the polymer chains were) and correlation length (ξ, used to determine polymer bundle separations and network mesh size as appropriate) were calculated (SI Table 3) and used to develop schematics for the gel structure (Fig. 2b,d,f,h).

Scattering plots for [emim][OAc] and [emim][$EtSO_4$] (where deuterated [emim][$MeSO_4$] was used as a proxy) gels all showed similar profiles with steep scattering at low q (Fig. 2a,c). In all cases, the porod exponent was around 4 (SI Table 3), indicating the presence of dense spherical bundles of crosslinked PEGDA. For these gels, the correlation length of the gels decreased with increasing polymer concentration (SI Table 3). In these cases, correlation length was an indicator of the distance between the dense polymer-rich regions, where separation decreased with increasing polymer content (Fig. 2b,d). Dense regions of polymer, where tightly coiled chains minimized crosslinking, was consistent with the low mechanical strength of the ionogels. In contrast to the [emim][OAc] gels, [emim][$EtSO_4$] ionogels displayed increased stiffness and toughness with increasing polymer loading compared to their [emim][OAc] counterparts (Fig. 1e). Similarly, the distance between the polymer bundles in [emim][$EtSO_4$] was moderately less

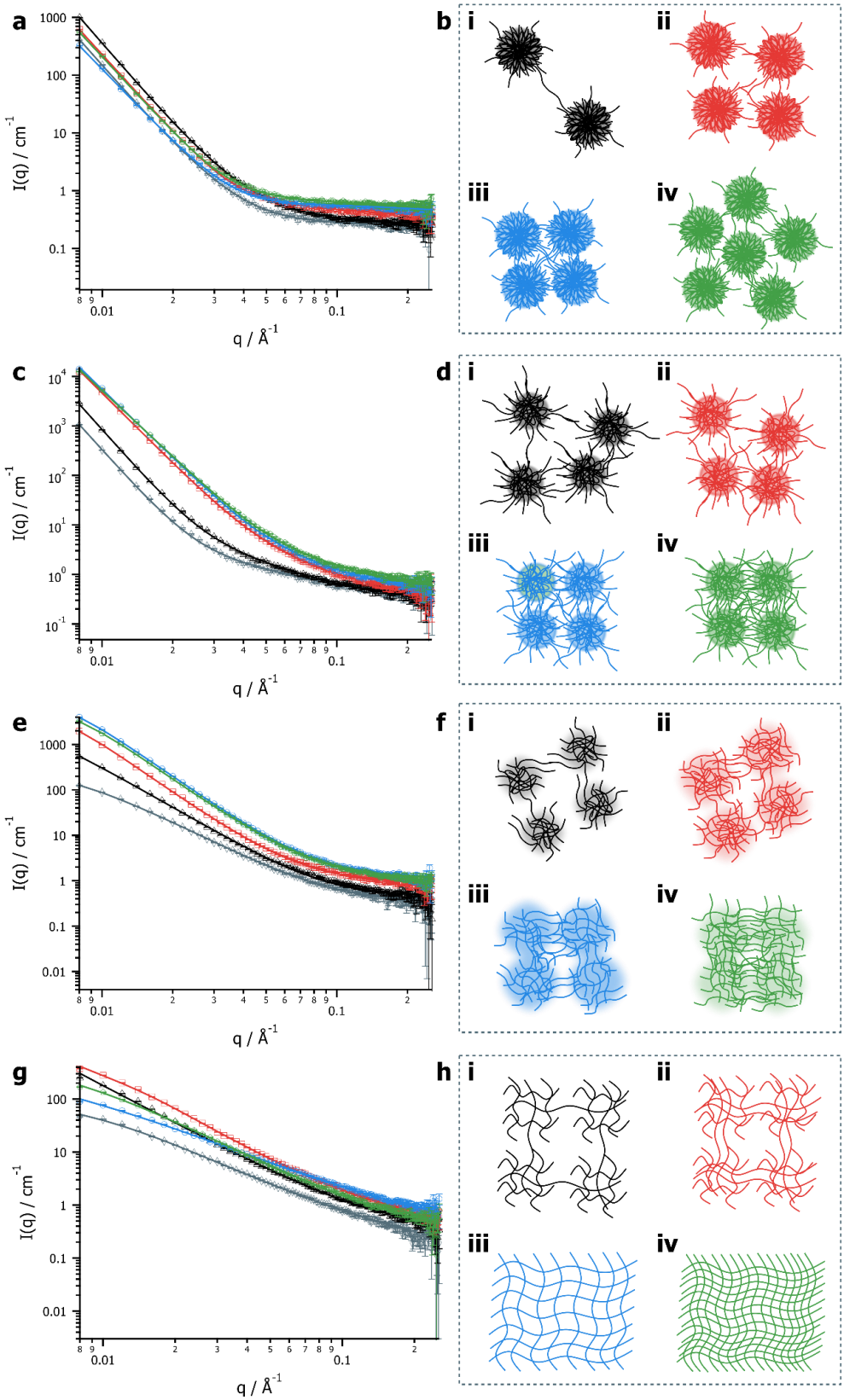

Figure 2. SANS profiles and corresponding schematic illustrations for ionogels of [emim][OAc] (**a**-**b**), [emim][$EtSO_4$] (**c**-**d**), [emim][OTf] (**e**-**f**), and [emim][NTf_2] (**g**-**h**) with 10 wt% (black triangles, **i**), 20 wt% (red squares, **ii**), 30 wt% (blue circles, **iii**), 40 wt% (green pentagons, **iv**), and 5 wt% solution (grey diamonds) for reference. Solid lines in SANS plots are correlation length fits.

sensitive to increasing polymer concentration. This suggested a slight increase in crosslinking in the [emim][$EtSO_4$] gels prevented the bundles getting as close as what was observed in [emim][OAc], and moderate network formation improved the mechanical strength as a result (Fig. 2d).

Whilst [emim][OAc] and [emim][$EtSO_4$] ionogels displayed very similar mechanical properties and scattering profiles, this was not the case for the [emim][OTf] and [emim][NTf_2] gels. For these gels, SANS profiles (Fig. 2e,g) showed porod exponents in the range 2 – 3, indicating that these ionic liquids were better solvents, with PEGDA now forming highly crosslinked fractal networks, as opposed to loosely connected regions of polymer. This served as further evidence towards anion basicity playing a pivotal role in gel properties, in this case through the structuration of polymers (as evidenced through the porod exponent).

For [emim][OTf], the scattering profile for the pre-gel concentration of PEGDA (5 wt%) had a porod exponent of 2.06 and correlation length of 142.5 Å (Fig. 2e), indicating that the ionic liquid was acting as a θ-solvent, with the polymer now in an extended conformation. Similarly, in [emim][NTf_2], the 5 wt% pre-gel solution showed a porod exponent of 1.47, indicating good solvent conditions (Fig. 2g). When the polymer concentration was increased to 10 wt%, the concentration required for a free-standing gel, for both [emim][OTf] and [emim][NTf_2], there were increases in the correlation length (SI Table 3), indicative towards the polymer forming loose networks of fractal objects. Given the similar mechanical properties to the equivalent [emim][OAc] and [emim][EtSO4] gels, this suggested the presence of low density regions of polymer that were loosely connected (Fig. 2f,h). When the polymer content was increased to 20 wt%, in [emim][OTf] the porod exponent increased to 2.3 and correlation length decreased to 187.2 Å, indicating that the polymers were beginning to form a much more fractal network. However, in light of the mechanical properties, this suggested the presence of some entangled bundles of polymer persisting (Fig. 2f,ii). By comparison, for [emim][NTf_2] the correlation length increased moderately to 142.3 Å concomitant with a decrease in porod exponent to 1.81. This indicated that the regions of polymer were becoming more crosslinked with greater network formation (Fig. 2h,ii). This increased network was in agreement with the significant 4-fold increase in the stiffness moving from a concentration of 10 wt% to 20 wt% (SI Table 2).

At 30 wt% the polymer concentration was now high enough for a considerable amount of crosslinking and network formation in both [emim][OTf] and [emim][NTf_2] (Fig. 2f,h). This switch from loosely associated bundles of polymer to a network of polymer was reflected in the mechanical properties, with significant increases in the compressive modulus of these gels compared to their [emim][OAc] and [emim][$EtSO_4$] equivalents (SI Table 2). This was particularly prevalent for the [emim][NTf_2] gels, where a porod exponent of 1.58 and scattering length of 175.0 Å (Fig. 2g, SI Table 3), indicated extended polymer chains, behaving as ideal solutes, forming extended mesh-like networks (Fig. 2h,iii). This was in broad agreement with the mechanical properties, which showed that the [emim][NTf_2] and [emim][OTf] gels were the stiffest and toughest of all the gels tested (Fig. 1e, SI Table 2).

When the PEGDA concentration was increased to 40 wt%, the density of the polymers increased, evidenced through the slight increases in the porod exponent and further decreases in the correlation length (SI Table 3). For the [emim][OTf] ionogel this was in agreement with the increase in stiffness and toughness. Overall, these observations indicated that the structure of the [emim][OTf] 40 wt% crosslinked PEGDA gel was that of a dense fractal network of polymer (Fig. 2f,iv). Whilst this was broadly the same for the [emim][NTf_2] gel, in this case the

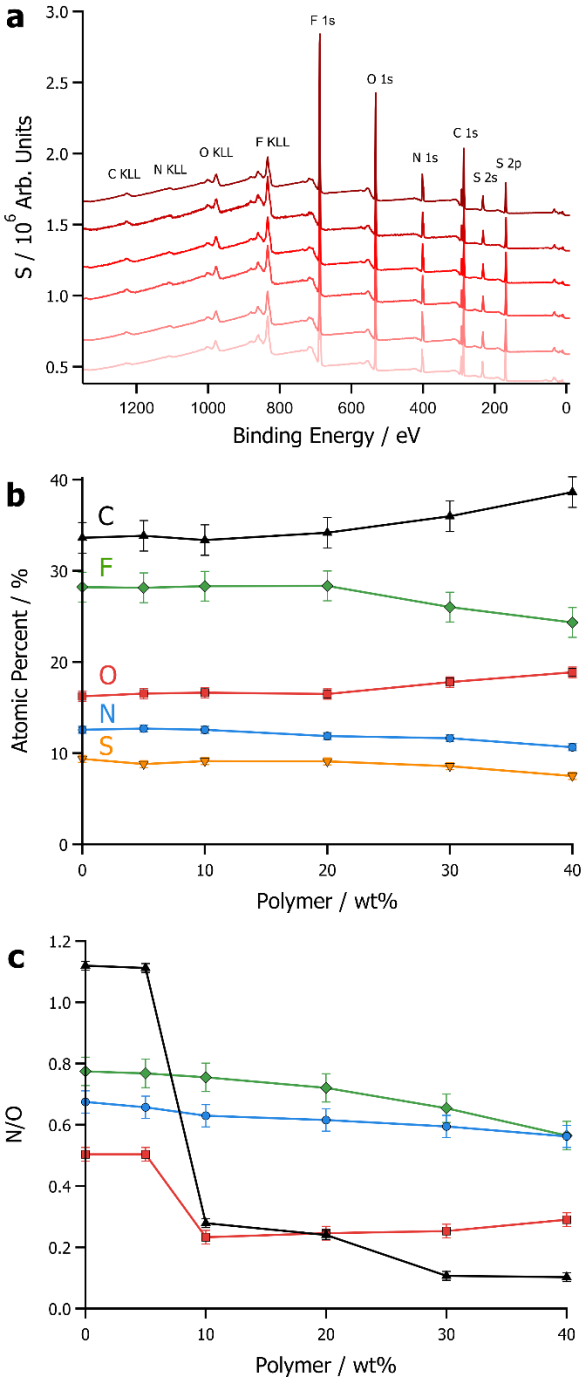

Figure 3. (**a**) XPS survey scan for ionogels of [emim][NTf_2] and crosslinked PEGDA at 0, 5, 10, 20, 30, and 40 wt% (pink – dark red). (**b**) Plot of atomic percent against PEGDA concentration for [emim][NTf_2] ionogels (calculated from survey scan shown in Fig. 3a). (**c**) Plot of the ratio of N to O (as calculated from atomic % data derived from XPS scans – Fig. 3a, SI Fig. 1, SI Table 4) against PEGDA concentration for ionogels with [emim][OAc] (black triangles), [emim][$EtSO_4$] (red squares), [emim][OTf] (blue circles), and [emim][NTf_2] (green diamonds). N/O was chosen as a proxy to monitor the IL:PEGDA ratio.

polymer packing was such that any gains in stiffness was negated by a significant increase in brittleness – where the failure strain was reduced dramatically from 48 % to 27 % (SI Table 2). This was reflected in the scattering data (Fig. 2g), which showed a slight contraction in correlation length (from 175.0 Å to 138.2 Å) that was concomitant with an increase in the porod exponent (from 1.58 to 1.93, SI Table 3), indicating a formation of a much denser network of polymer (Fig. 2h,iv).

Overall, SANS profiles provided structural information on the various ionogels, which could be correlated to their mechanical properties. Particularly, deciphering the polymer behaviour in the ionogels revealed that, in line with the mechanical properties, decreasing the polarity of the ionic liquid increased its solvent potential with respect to PEGDA. This demonstrated that the physical properties of ionogels could be specifically tuned through choice of ionic liquid, explained in-turn by the arrangement and structure of the polymers within the solvent.

The negligible vapour pressure of ionic liquids provided a unique opportunity to study the surface composition of the ionogels, something that is not feasible for other gel systems as vaporisation of the solvent makes these experiments otherwise impossible to conduct. To complement our SANS structural studies, XPS was used to investigate the molecular species present at the ionogel surface (Fig. 3, SI Fig. 1-2, SI Table 4). XPS survey scans (Fig. 3a, SI Fig. 1) were used to calculate the atomic content of the ionogel surfaces (Fig. 3b, SI Fig. 2, SI Table 4). For all ionogels, as the polymer content was increased, signals associated predominately with the ionic liquid (S, N, F) decreased concomitantly with increases in the signals associated primarily with PEG (C, O). As expected, this indicated an increasing polymer composition at the ionogel surface and a decreasing ionic liquid composition. However, there were striking differences between the modality of this change between ionic liquids. To simplify the analysis, the atomic ratio of N to O (N/O) was chosen as a proxy to express ionic liquid to polymer ratio at the sample surface (Fig. 3c). This was validated through the S/N ratio (SI Fig. 3), which was consistent at all polymer concentrations, indicating that observations were not due to cation and anion segregation at the ionogel surface. For ionogels of both [emim][OAc] and [emim][$EtSO_4$], when the crosslinked PEGDA concentration was increased to the minimum required for gelation (10 wt%), there was a significant decrease in the N/O ratio indicating the sudden appearance of a polymer rich surface. The ionic liquid content at the surface of the ionogel was significantly lower than within the bulk, suggesting a lack of cohesion between ionic liquid and polymer-rich domains. This was entirely consistent with both the bulk structure (large spherical objects that were loosely connected), and the comparatively low mechanical strength. Conversely, when the ionic liquid was either [emim][OTf] or [emim][NTf_2], the decrease in N/O with increasing polymer content was much more gradual. This suggested that there was minimal segregation of ionic liquid between the bulk and the surface, as compared to the [emim][OAc] and [emim][$EtSO_4$] gels. Again, this was in agreement with the SANS data and served as further evidence to the presence of uniform polymer networks throughout these ionogels.

Conclusions

Ionic liquids have emerged as highly tuneable solvents for use in the development of functional materials. Taking advantage of their unusual solvent properties, we have deployed a combination of analytical techniques that have not been used on gel systems before. Specifically, SANS and XPS have provided a glimpse into structure-property relationships that would not otherwise be possible in volatile solvents. Drawing from these experiments, we have shown that the physical properties of ionogels are entirely dependent on both the ionic liquid component and polymer content. Further, we have demonstrated that the structural motifs of the gels – both within the bulk and at the surface – changes considerably with ionogel composition. The defining features being tight compact polymer rich regions in the more polar ionic liquids, moving towards extended networks in the less polar ionic liquids where polymer-solvent interactions are more favourable. Through consideration of the polarity of the ionic liquid anion, ionogels possess an extra level of tuneability compared to analogous gels of other solvents. As such, the results presented here illustrate that through systematic SANS and XPS studies, the modularity of ionogels is intrinsically linked to the structure of the polymer, which in turn is controlled by the tuneable solvent capability of the ionic liquid. As a result, we provide a framework for understanding – and expanding – the design space of gel materials. It is obvious that the research presented here only begins to probe the boundaries of ionogel design. Therefore, subsequent research will do well to build on these foundations, and explore the vast variety of components available (and their combinations), including those that are biologically compatible, polymers that are environmentally responsive, and deep eutectic solvents. Furthermore, as the physical properties examined here will impact charge transport within the gels, studying conductivity as a function of ionogel structure (both bulk and surface) will be of great importance. The result will be a structure-led consideration for the careful development of functional gels, opening avenues towards a plethora of new applications.

Conflicts of interest

There are no conflicts to declare.

Acknowledgements

The authors would like to thank EPSRC (Frontier Engineering Grant EP/K038648/1) for providing funding for this work, and for STFC/ISIS Neutron and Muon Source for granting access to LOQ and providing the deuterated resources to perform the SANS experiments. We also thank Dr. Ruth Brooker for access to the Instron 5543.

Notes and references

1 J. P. Hallett and T. Welton, *Chem. Rev.*, 2011, **111**, 3508–76.
2 C. J. Clarke, W.-C. Tu, O. Levers, A. Bröhl and J. P. Hallett, *Chem. Rev.*, 2018, **118**, 747–800.
3 P. C. Marr and A. C. Marr, *Green Chem.*, 2015, **18**, 105–108.
4 A. Vioux, L. Viau, S. Volland and J. Le Bideau, *C. R. Chim.*, 2010, **13**, 242–255.
5 J. Le Bideau, L. Viau and A. Vioux, *Chem. Soc. Rev.*, 2011, **40**, 907–925.
6 A. J. D'Angelo and M. J. Panzer, *Adv. Energy Mater.*, 2018, **8**, 1–13.
7 Y. Cao, T. G. Morrissey, E. Acome, S. I. Allec, B. M. Wong, C. Keplinger and C. Wang, *Adv. Mater.*, 2017, **29**, 1605099.
8 H. Qin and M. J. Panzer, *ChemElectroChem*, 2017, **4**, 2556–2562.
9 Y. Ding, J. Zhang, L. Chang, X. Zhang, H. Liu and L. Jiang, *Adv. Mater.*, 2017, **29**, 1704253.
10 S. Z. Bisri, S. Shimizu, M. Nakano and Y. Iwasa, *Adv. Mater.*, 2017, **29**, 1607054.
11 A. J. D'Angelo, J. J. Grimes and M. J. Panzer, *J. Phys. Chem. B.*, 2015, **119**, 14959–14969.
12 N. Buchtová, A. Guyomard-Lack and J. Le Bideau, *Green Chem.*, 2014, **16**, 1149–1152.
13 B. Chen, J. J. Lu, C. H. Yang, J. H. Yang, J. Zhou, Y. M. Chen and Z. Suo, *ACS Appl. Mater. Interfaces*, 2014, **6**, 7840–7845.
14 A. F. Visentin, S. Alimena and M. J. Panzer, *ChemElectroChem*, 2014, **1**, 718–721.
15 P. Vidinha, N. M. T. Lourenço, C. Pinheiro, A. R. Brás, T. Carvalho, T. Santos-Silva, A. Mukhopadhyay, M. J. Romão, J. Parola, M. Dionisio, J. M. S. Cabral, C. A. M. Afonso and S. Barreiros, *Chem. Commun.*, 2008, **44**, 5842–5844.
16 A. P. S. Brogan and J. P. Hallett, *J. Am. Chem. Soc.*, 2016, **138**, 4494–4501.
17 A. P. S. Brogan, L. Bui-Le and J. P. Hallett, *Nat. Chem.*, 2018, **10**, 859–865.
18 H. Srour, M. Leocmach, V. Maffeis, A. C. Ghogia, S. Denis-Quanquin, N. Taberlet, S. Manneville, C. Andraud, C. Bucher and C. Monnereau, *Polym. Chem.*, 2016, **7**, 6608–6616.
19 T. Masuda, T. Ueki, R. Tamate, K. Matsukawa and R. Yoshida, *Angew. Chem. Int. Ed.*, 2018, **57**, 16693–16697.
20 Z. Sun, Y. Yamauchi, F. Araoka, Y. S. Kim, J. Bergueiro, Y. Ishida, Y. Ebina, T. Sasaki, T. Hikima and T. Aida, *Angew. Chem. Int. Ed.*, 2018, **57**, 15772–15776.
21 J. Chen, F. Xie, L. Chen and X. Li, *Green Chem.*, 2018, **20**, 4169–4200.
22 M. A. Ab Rani, A. Brant, L. Crowhurst, A. Dolan, M. Lui, N. H. Hassan, J. P. Hallett, P. A. Hunt, H. Niedermeyer, J. M. Perez-Arlandis, M. Schrems, T. Welton and R. Wilding, *Phys. Chem. Chem. Phys.*, 2011, **13**, 16831–16840.
23 A. F. M. Cláudio, L. Swift, J. P. Hallett, T. Welton, J. A. P. Coutinho and M. G. Freire, *Phys. Chem. Chem. Phys.*, 2014, **16**, 6593–601.
24 T. Ueki and M. Watanabe, *Bull. Chem. Soc. Jpn.*, 2012, **85**, 33–50.
25 H.-N. Lee and T. P. Lodge, *J. Phys. Chem. Lett.*, 2010, **1**, 1962-1966.
26 R. J. Sengwa, K. Kaur and R. Chaudhary, *Polym. Int.*, 2000, **49**, 599–608.
27 P. K. Pandey, K. Rawat, V. K. Aswal, J. Kohlbrecher and H. B. Bohidar, *Phys. Chem. Chem. Phys.*, 2016, **19**, 804–812.
28 K. Hashimoto, K. Fujii, K. Nishi and M. Shibayama, *J. Phys. Chem. B.*, 2018, **122**, 9419–9424.
29 K. Fujii, H. Asai, T. Ueki, T. Sakai, S. Imaizumi, U. Chung, M. Watanabe and M. Shibayama, *Soft Matter*, 2012, **8**, 1756–1759.